

The case of the biased quenched trap model in two dimensions with diverging mean dwell times.

Dan Shafir* and Stanislav Burov†

Physics Department, Bar-Ilan University, Ramat Gan 5290002, Israel

(Dated: January 17, 2022)

Abstract

We investigate the biased quenched trap model on top of a two-dimensional lattice in the case of diverging expected dwell times. By utilizing the double-subordination approach and calculating the return probability in 2d, we explicitly obtain the disorder averaged probability density function of the particle's position as a function of time (for any given bias) in the limit of large times ($t \rightarrow \infty$). The first and second moments are calculated, and a formula for a general μ -th moment is found. The behavior of the first moment, i.e. $\langle x(t) \rangle$, presents non-linear response both in time and in the applied external force F_0 . While the non-linearity in time occurs for any measurement time t , the non-linearity in F_0 is expected only when $t \gtrsim (F_0 |\ln(F_0)|)^{-2/\alpha}$ where $\alpha = T/T_g$, for temperatures $T < T_g$. We support our analytic results by comparison to numerical simulations.

* dansh5d@gmail.com

† stasbur@gmail.com

I. INTRODUCTION

Properties of transport in a disordered medium where the motion is dictated by diverging expected waiting (or dwell) times have been the subject of rigorous research in many fields [1–3]. Such systems exhibit anomalous slow diffusion, termed subdiffusion, i.e the second moment grows with time as $\langle x^2(t) \rangle \sim t^\alpha$ where $0 < \alpha < 1$. This type of diffusion describes motion in complex disordered systems such as living cells [4, 5], blinking quantum dots [6], molecular-motor transport on a filament network [7] and photocurrents in amorphous materials [8]. It was also shown that anomalous diffusion could be used to describe the aging phenomenon in glasses [9–13].

The basic model to describe transport in disordered material is the random walk (RW) on a lattice. One of the most popular generalizations of the RW is the continuous-time random walk (CTRW) that was developed in the works of Montroll, Scher, and others [8, 14–16] as a description of transport in amorphous materials. CTRW describes the motion of a traced particle affected by traps. The particle can be trapped in various locations of the media, where it waits for some random time before continuing its motion. In CTRW, the particle hops from site to site on top of a lattice. Between the hops, a random dwell time is generated. When the expected dwell times diverge, the behavior is non-ergodic [17, 18] and subdiffusive. The dwell times between hops for a CTRW process on top of a lattice are assumed to be independent, identically distributed (i.i.d) random variables. This situation of uncorrelated disorder is termed annealed disorder, and it allows mathematical treatment utilizing the renewal theory. The disorder when the dwell times are position-dependent is termed quenched disorder. In the quenched trap model (QTM), the dwell time at each lattice site stays fixed for the whole time. This means that if the particle revisits the same site, it stays there for the same dwell time as during the previous visitation.

For quenched disorder, the renewal assumption is lost, at least below a critical dimension, since revisiting a site invokes previously experienced dwell time. Nevertheless, scaling arguments and the renormalization group approach [2, 19, 20] suggests that for dimension $d > 2$, QTM behaves like CTRW, which in some sense represents a mean-field approximation for the QTM. In [21–24] a similar conclusion was obtained by using a rigorous mathematical description of QTM on a regular lattice and a more general approach of randomly trapped random walks. The correspondence between QTM and CTRW is exact when $d \rightarrow \infty$. The logic behind this claim stems from the fact that in high dimensions ($d > 2$), the particle is non-recurrent and rarely visits the same site more than once. So by increasing the dimensionality, we reduce our correlations and approach the annealed case of CTRW. Below the critical dimension of 2 (the particle is recurrent), correlations imposed by identical dwell times become apparent and cannot be ignored. Thus, when considering an RW in a system with quenched disorder, correlations in space (due to multiple visits to the same site) make the RW much harder to handle mathematically.

While an abundance of research on the subject at hand is present, a direct mapping between QTM and CTRW has been lacking until recently. Recent works [25, 26] have shown that a temporal transformation can take us from CTRW to the equivalent time in QTM, in the case of transient RW where the probability of return to a previously visited site (Q_0) is less than 1. Specifically, this temporal transformation is valid for systems with dimension $d > 2$ or any biased walk (i.e. external force is applied) with quenched trapping disorder [27–30]. This mapping between CTRW and QTM was the result of introducing a new local time parameter (S_α), which allowed to calculate the QTM’s spatial probability density function (PDF), averaged over disorder, for the biased one-dimensional case [26]. The QTM’s PDF of the particle’s position on top of a two-dimensional lattice has yet to be found and compared to numerical results. Hence the purpose of this paper.

While the one-dimensional and two-dimensional situations share similar features, like the infinite average number of steps it takes the particle to return to the origin, these cases are qualitatively different. To better understand the difficulties caused by working in two dimensions, we mention a problem discussed by Weiss [31]. Consider a set of k ($k > 0$) independent non-interacting walkers. Each performing unbiased RW, and all are starting from the same starting position simultaneously. Assuming that the RW is recurrent, we consider the average return time of the earliest walker to return to the origin. The question is, how large k has to be to ensure that the first one to return to the origin has a finite average return time? In $1d$, the answer is $k > 2$, and in fact, the first $(k - 2)$ returning RWs will have a finite average return time. For the two-dimensional case, for any $k > 0$, none of the walkers will have a finite average return time. This result emphasizes the difficulty of working in two dimensions. Therefore the properties of quenched disorder in two-dimensional QTM need to be handled with much care.

This paper is organized in the following manner. In Sec. (II), we provide a brief review of the theoretical background and a formula for the μ -th moment of the position, together with the particle's diffusion front. In Sec. (III), we explicitly evaluate the first and second moments which exhibit anomalous diffusion and non-linear response for the case of the rectangular lattice. In the appendix (VII), we provide examples for the evaluation of the moments on other lattice types, such as the oblique and hexagonal lattices. Sec. (V) presents the equivalency between the QTM and CTRW. A temporal mapping between the two is given, and a comparison between QTM in one and two dimensions is performed. In Sec. (IV) we discuss the simulations and validate our theoretical results. A formula for the minimal measurement time required for the theory and simulations to converge is achieved. Sec. (VI) presents our conclusions and relates our results to other works done in the field.

II. THEORETICAL BACKGROUND

For the CTRW model with diverging mean dwell-times, the process is decomposed into ordinary spatial Brownian motion and a temporal Lévy process, an approach called subordination [32–36]. In QTM, the disorder is quenched, the dwell times are correlated, and Lévy’s limiting theorem cannot be applied since the dwell times are not i.i.d. To solve this problem, we follow recent works [25, 26, 37, 38] and define a new local time parameter together with an approach termed double subordination to solve a biased QTM on a 2d lattice with diverging mean dwell times. As was mentioned in Ref. [25] when QTM is biased, the return probability is < 1 , the quenched nature of QTM is less apparent (fewer re-visitations of lattice sites), and one can assert those correlations imposed by the quenched dwell times can be effectively renormalized into uncorrelated times, i.e., a CTRW description. Thus a mapping between QTM and CTRW can be achieved. In this section, we summarize the results received in a recent paper by one of the authors [26] and expand upon them in the following sections to obtain the moments for the case of the transient (nonrecurring) QTM affected by a bias in two dimensions. We refer the interested reader to the original paper [26] for rigorous derivations.

Our first step is to define the problem and present the local time used in the case of the quenched disorder. Before doing that, to better understand the thought process, we will show why the local time in the case of CTRW (annealed disorder) is simply the number of jumps N . For a given number of waiting times N , the total measurement time t is

$$t = \sum_{i=1}^N \tau_i \quad (1)$$

where τ_i are the local dwell times, i.e., i.i.d random variables distributed according to the PDF $\omega(\tau_i) = A\tau_i^{-(1+\alpha)}/|\Gamma(-\alpha)|$ where $0 < \alpha < 1$, $A > 0$ and $\Gamma()$ is the Gamma

function. For these values of α , the average of each τ_i is diverging. It is known [2] that in the large N limit

$$\text{PDF} \left(\frac{t}{N^{1/\alpha}} \right) = l_{\alpha,A,1} \left(\frac{t}{N^{1/\alpha}} \right) \quad (2)$$

where $l_{\alpha,A,1}()$ is the one sided Lévy distribution [38] which is defined by its Laplace transform, $\int_0^\infty e^{-Zu} l_{\alpha,A,1}(Z) dZ = e^{-Au^\alpha}$. We now have the probability of observing t for a given number of steps N . Then, the probability of observing N steps during time t can be found [2, 26] by changing variables from $Z = t/N^{1/\alpha}$ to $N = (t/Z)^\alpha$ with the result

$$\mathcal{P}_t(N) = \frac{t}{\alpha} N^{-1-1/\alpha} l_{\alpha,A,1} \left(\frac{t}{N^{1/\alpha}} \right) \quad (t \rightarrow \infty). \quad (3)$$

We condition on the different outcomes of N (in the limit of $t \rightarrow \infty$) and obtain for the PDF to observe a particle in position \mathbf{r} at time t ,

$$\langle P(\mathbf{r}, t) \rangle_{CTRW} = \sum_N W_N(\mathbf{r}) \mathcal{P}_t(N), \quad (4)$$

where $\langle \dots \rangle$ is an average upon disorder (many realizations) and $W_N(\mathbf{r})$ is the PDF of regular RW irrespective of the various dwell times, i.e can be approximated by a Gaussian in the large N limit (by using the central limit theorem). Eq. (4) shows that since in the PDF of the regular RW, i.e., $W_N(\mathbf{r})$, the time is replaced by N , hence N is the natural choice for the local time in the case of CTRW. This procedure of separating CTRW into spatial and temporal processes is termed subordination.

Now we return to our main subject of the QTM and apply a similar approach by finding the appropriate local time. During the measurement time t , the particle has visited a certain amount of lattice points and stayed exactly $\tau_{\mathbf{r}}$ at each lattice point \mathbf{r} . The quenched dwell times $\tau_{\mathbf{r}}$ are real, positive, and independently distributed random variables with

$$\psi(\tau_{\mathbf{r}}) \sim \tau_{\mathbf{r}}^{-(1+\alpha)} A / |\Gamma(-\alpha)| \quad (\tau_{\mathbf{r}} \rightarrow \infty) \quad (5)$$

as the PDF ($A > 0$ and $\Gamma()$ is the Gamma function). The value of the exponent α is bounded to $0 < \alpha < 1$. For these values of α , the average dwell times diverge, i.e., $\langle \tau_{\mathbf{r}} \rangle = \int_{\tau_{min}}^{\infty} \tau_{\mathbf{r}} \psi(\tau_{\mathbf{r}}) d\tau_{\mathbf{r}} = \infty$ and the model results in anomalous sub-diffusion and aging [9]. The physical representation of QTM assumes a thermally activated particle that is jumping between various energetic traps. When the particle is in a trap located at \mathbf{r} , the mean escape time $\tau_{\mathbf{r}}$ is given by Arrhenius law $\tau_{\mathbf{r}} \sim \exp(E_{\mathbf{r}}/T)$, where $E_{\mathbf{r}}$ is the depth of the trap and T is the temperature. When the PDF of $E_{\mathbf{r}}$ is exponential, i.e., $\frac{1}{T_g} \exp(-E_{\mathbf{r}}/T_g)$, the mean escape time achieves a PDF in the form of $\psi(\tau_{\mathbf{r}})$ where $\alpha = T/T_g$. For low temperatures ($T < T_g$), one observes glassy behavior (aging and non-self averaging) in the system [39].

The measurement time t is provided by

$$t = \sum_{i=0}^N \tau_i = \sum_{\mathbf{r}} n_{\mathbf{r}} \tau_{\mathbf{r}} \quad (6)$$

where $n_{\mathbf{r}}$ is the number of times the particle visited site \mathbf{r} during t and the summation is over all the lattice points. In the case of QTM, the quantity

$$S_{\alpha} = \sum_{\mathbf{r}} (n_{\mathbf{r}}(t))^{\alpha} \quad (7)$$

can serve as the local time in the same way that the number of jumps N (performed during the time t) is the local time for CTRW. This is true based on the fact that in the limit of $t \rightarrow \infty$

$$\text{PDF} \left(\frac{t}{S_{\alpha}^{1/\alpha}} \right) = l_{\alpha,A,1} \left(\frac{t}{S_{\alpha}^{1/\alpha}} \right) \quad (8)$$

which was proven in [25, 26, 37]. Eq. (8) is the QTM's analog of the CTRW (Eq. (2)) where we have switched the local time N with S_{α} . Note that S_{α} is a spatial variable that depends solely on various positions of the particle and not the time spent at those sites. For $\alpha = 1$ S_{α} is the total number of steps performed, and for $\alpha = 0$ is the total number of distinct sites visited during t .

The probability of observing a specific S_α for a given measurement time t (i.e., $\mathcal{P}_t(S_\alpha)$) is now obtained from Eq. in a similar fashion to how Eq. (3) was obtained from the relation in Eq. (2) [26]:

$$\mathcal{P}_t(S_\alpha) \sim \frac{t}{\alpha} S_\alpha^{-1/\alpha-1} l_{\alpha,A,1} \left(\frac{t}{S_\alpha^{1/\alpha}} \right) \quad (t \rightarrow \infty). \quad (9)$$

The PDF $P(\mathbf{r}, t)$ to find the particle at position \mathbf{r} after measurement time t is calculated by conditioning on all the possible S_α that can occur during the process. One needs to sum over all the possible $P_{S_\alpha}(\mathbf{r})$ (i.e. the PDF to observe the particle at \mathbf{r} for a given S_α) multiplied by the appropriate probability to observe such S_α at time t , for a given disorder. After averaging over disorder, the PDF takes the form

$$\langle P(\mathbf{r}, t) \rangle = \sum_{S_\alpha} P_{S_\alpha}(\mathbf{r}) \mathcal{P}_t(S_\alpha) \quad (10)$$

and due to Eq. (9), in the $t \rightarrow \infty$ limit we obtain

$$\langle P(\mathbf{r}, t) \rangle \sim \int_0^\infty P_{S_\alpha}(\mathbf{r}) \frac{t}{\alpha} S_\alpha^{-1/\alpha-1} l_{\alpha,A,1} \left(\frac{t}{S_\alpha^{1/\alpha}} \right) dS_\alpha \quad (11)$$

The PDF $P(\mathbf{r}, t)$ depends on $P_{S_\alpha}(\mathbf{r})$. The form of $P_{S_\alpha}(\mathbf{r})$ is obtained by using again the subordination approach where the local time S_α is subordinated to N , number of jumps performed, and the spatial process is provided by $W_N(\mathbf{r})$ —the PDF of regular RW, i.e.

$$P_{S_\alpha}(\mathbf{r}) = \sum_{N=0}^{\infty} W_N(\mathbf{r}) \mathcal{G}_{S_\alpha}(N, \mathbf{r}) \quad (12)$$

where $\mathcal{G}_{S_\alpha}(N, \mathbf{r})$ is the probability to perform N steps before reaching \mathbf{r} provided that the value of S_α is known.

Now we need to find an explicit expression for $P_{S_\alpha}(\mathbf{r})$ to establish a simplified representation of the positional PDF, i.e. $P(\mathbf{r}, t)$. From [25, 26] we know that for the case when the spatial process is transient and the probability of eventually returning

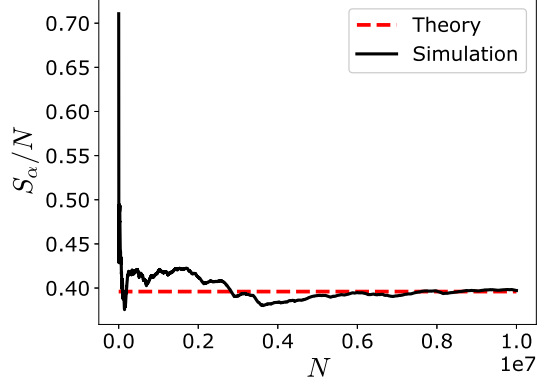


FIG. 1: An example for the convergence of $S_\alpha(N)$ to ΛN for the case of a two-dimensional RW on a square lattice (with unit spacing), $\alpha = 0.5$. The external force is $\vec{F} = 0.001(\hat{x} + \hat{y})$ which means, following Eq. (38), that the return probability $Q_0 = 0.812979$. The thick line represents the simulation while the dashed line is the theoretical limit provided by Eq. (14).

to the origin Q_0 , is less than 1, in the large N limit, the local time S_α and the number of jumps N obey linear dependence

$$\langle S_\alpha(N) \rangle = \Lambda N \quad (N \rightarrow \infty) \quad (13)$$

where

$$\Lambda = \frac{(1 - Q_0)^2}{Q_0} Li_{-\alpha}(Q_0) \quad (14)$$

and $Li_a(b) = \sum_{j=1}^{\infty} b^j / j^a$ is the Polylogarithm function. Moreover, it was proven in detail in Ref. [26] that for any value of \mathbf{r}

$$\mathcal{G}_{S_\alpha}(N, \mathbf{r}) \xrightarrow{S_\alpha \rightarrow \infty} \delta(S_\alpha - \Lambda N). \quad (15)$$

This result stems from the fact that $\langle S_\alpha \rangle \rightarrow \Lambda N$ while also $\text{Var}(\langle S_\alpha \rangle) \rightarrow 0$. An example for the convergence of S_α/N to Λ can be observed in Fig. 1. By plugging

Eq. (12) into Eq. (10) we perform a **double subordination** that prescribes the disorder averaged PDF $\langle P(\mathbf{r}, t) \rangle$ the form

$$\langle P(\mathbf{r}, t) \rangle = \sum_{S_\alpha} \sum_{N=0}^{\infty} W_N(\mathbf{r}) \mathcal{G}_{S_\alpha}(N, \mathbf{r}) \mathcal{P}_t(S_\alpha). \quad (16)$$

Note that by taking the limit, $t \rightarrow \infty$, only large S_α need to be considered. In addition, the regular practice of the subordination technique is to replace the sums in (16) by integrals [2]. Therefore, by substituting the value for $\mathcal{G}_{S_\alpha}(N, \mathbf{r})$ from Eq. (15), the form of $\mathcal{P}_t(S_\alpha)$ in Eq. (9) finally gives us the expression for the positional PDF

$$\langle P(\mathbf{r}, t) \rangle \sim \int_0^\infty W_N(\mathbf{r}) \frac{t/\Lambda^{1/\alpha}}{\alpha} N^{-1/\alpha-1} l_{\alpha,A,1} \left(\frac{t/\Lambda^{1/\alpha}}{N^{1/\alpha}} \right) dN \quad t \rightarrow \infty \quad (17)$$

By acquiring the positional PDF we can now calculate any moment μ of the QTM, i.e., $\langle |\mathbf{r}|^\mu \rangle$ by its definition,

$$\langle |\mathbf{r}|^\mu \rangle_{\text{QTM}} = \int |\mathbf{r}|^\mu \langle P(\mathbf{r}, t) \rangle d\mathbf{r}. \quad (18)$$

Since the positional PDF is a function of the displacement (\mathbf{r}) and the number of steps N , we can evaluate the displacement dependent part of the function separately. This part happens to be the moments of regular RW,

$$\langle |\mathbf{r}|^\mu \rangle_{\text{RW}} = \int |\mathbf{r}|^\mu W_N(\mathbf{r}) d\mathbf{r} = \sum_{i=1}^{\mu} B_\mu^{(i)} N^{\gamma_\mu^{(i)}}. \quad (19)$$

The right-hand side of Eq. (19) is the general solution of the μ -th moment with the constants B_μ and γ_μ which depend on the bias (force) and the lattice type (including dimension). In the next section, we will explicitly evaluate these constants for square and rectangular lattices. In the appendix, we consider other examples - the oblique and hexagonal lattice types. Eq. (19) can be evaluated using the central limit

theorem. In the limit of large N the positional PDF $W_N(\mathbf{r})$ of a regular RW after N steps attain the Gaussian form

$$W_N(\mathbf{r}) = \frac{1}{\sqrt{2\pi N \text{Var}(l)^2}} \exp \left[-\frac{(\mathbf{r} - \langle l \rangle N)^2}{2N \text{Var}(l)^2} \right] \quad (20)$$

with single-step displacement $\langle l \rangle$ and variance $\text{Var}(l)$. Now all the moments of regular RW can be easily computed. Then according to Eq. (17), the μ th moment for the QTM is provided by substituting Eq. (19) into Eq. (18) with the general result

$$\langle |\mathbf{r}|^\mu \rangle_{\text{QTM}} = \sum_{i=1}^{\mu} \int_0^{\infty} (B_\mu^{(i)} t / \Lambda^{1/\alpha} \alpha) N^{\gamma_\mu^{(i)} - 1 - 1/\alpha} l_{\alpha, A, 1}(t / (\Lambda N)^{1/\alpha}) dN \quad (21)$$

and utilizing the identity [33]

$$\int_0^{\infty} y^q l_{\alpha, A, 1}(y) dy = A^{q/\alpha} \Gamma[1 - q/\alpha] / \Gamma[1 - q], \quad (q/\alpha < 1) \quad (22)$$

the expression for the moments of \mathbf{r} takes the final form

$$\langle |\mathbf{r}|^\mu \rangle_{\text{QTM}} = \sum_{i=1}^{\mu} \frac{\Gamma[1 + \gamma_\mu^{(i)}]}{A^{\gamma_\mu^{(i)}} \Gamma[1 + \alpha \gamma_\mu^{(i)}]} \frac{B_\mu^{(i)}}{\Lambda^{\gamma_\mu^{(i)}}} t^{\alpha \gamma_\mu^{(i)}}. \quad (23)$$

The constants $\gamma_\mu^{(i)}$, $B_\mu^{(i)}$ and Λ (which is determined by Q_0 through Eq. (14)) depend on the lattice dimension, force applied and the type of lattice. In the next section, we explicitly evaluate the first and second moments of the biased QTM model for a few two-dimensional lattice types.

III. RESPONSE TO A BIAS

In this section, we use the general form for the moments of \mathbf{r} as a function of measurement time (Eq. (23)) and evaluate the particular values of the first and second moments. We then utilize these quantities to explicitly obtain the response

to bias in QTM, i.e., the case when an external force is applied. In this section, we consider the rectangular and square lattice. Appendix (Sec. VII) shows how our approach can be extended to other lattice types, such as the oblique and hexagonal.

To calculate the moments of the QTM in Eq. (23), we need to find the constants $\gamma_\mu^{(i)}$, $B_\mu^{(i)}$ ($i = 1..\mu$) and Λ (which is determined by the return probability to a previously visited site Q_0). These constants are determined by the dimension, lattice type, and properties of the applied force. By applying a bias, i.e., a force F_0 , we modify the constants $B_\mu^{(i)}$ and the return probability Q_0 (which determines Λ in Eq. (23)). First we evaluate $\gamma_\mu^{(i)}$ and $B_\mu^{(i)}$ ($i = 1..\mu$) by calculating the moments of the spatial processes in Eq. (19), i.e regular RW on top of a lattice. We consider the case of a rectangular lattice with step size a in the x direction and b in the y direction. By setting $a = b$, we can easily find the case of the square lattice. We define q_{\rightarrow} and q_{\uparrow} to be the probability of the walker to take a step to the right (x axis) and upwards (y axis), respectively. The probabilities to jump to the left and downwards are then simply $q_{\leftarrow} = (1/2 - q_{\rightarrow})$ and $q_{\downarrow} = (1/2 - q_{\uparrow})$ respectively. So only two of the four jumping probabilities are required to define the problem. The external force F_0 is applied to the system at an angle θ (relative to the positive direction of the x axis). By applying a force, we change the hopping probabilities of the RW [39–41]. When the applied external force is sufficiency small (and independent of time), the jumping probabilities are proportional to $\exp(aF_x/2k_B T)$ and $\exp(bF_y/2k_B T)$ for a jump in the x direction and the y direction, respectively. Here k_B is Boltzmann’s constant, T is the temperature, F_x and F_y are the projections of the force on the x and y axis, i.e. $F_x = F_0 \cos(\theta)$ and $F_y = F_0 \sin(\theta)$. Since we are interested in the limit of small (and constant) force, the exponential contribution can be approximated to be linear by taking only the first two terms in Taylor’s series expansion. Hence the jumping

probabilities for a single step are

$$\begin{aligned}
q_{\rightarrow} &= \frac{1}{4}(1 + \tilde{F}_x) \\
q_{\uparrow} &= \frac{1}{4}(1 + \tilde{F}_y) \\
q_{\leftarrow} &= \frac{1}{4}(1 - \tilde{F}_x) \\
q_{\downarrow} &= \frac{1}{4}(1 - \tilde{F}_y)
\end{aligned} \tag{24}$$

where $\tilde{F}_x = aF_0 \cos(\theta)/(2k_B T)$ and $\tilde{F}_y = bF_0 \sin(\theta)/(2k_B T)$. Note that \tilde{F}_x and \tilde{F}_y are both dimensionless variables. By using the expressions for jumping probabilities, the moments of the horizontal position x can be obtained for the RW process on top of a rectangular lattice. We label these moments as $\langle x \rangle_{RW}$ and $\langle x^2 \rangle_{RW}$ with subscript RW to distinguish them from the QTM's moments (which will be labeled with a subscript of QTM). The average value of the RW's position \mathbf{r} after N steps can be found from the average value of a single step displacement l since $\langle \mathbf{r} \rangle_{RW} = \langle \sum_{i=1}^N l_i \rangle = N \langle l \rangle$ where l_i is the walker's displacement at step number i ($i \leq N$). The second moment is found by using the fact that the variance of \mathbf{r} can be deconstructed into a sum of the variances for different steps. This is true only when the steps are independent and uncorrelated. Hence the moments (say of x) of the spatial process are now

$$\langle x \rangle_{RW} = a(2q_{\rightarrow} - 0.5)N \tag{25}$$

$$\langle x^2 \rangle_{RW} = a^2 (0.5 - (2q_{\rightarrow} - 0.5)^2) N + a^2 (2q_{\rightarrow} - 0.5)^2 N^2 \tag{26}$$

Comparison of Eq. (19) to Eqs. (25,26) yields for $\gamma_{\mu}^{(i)}$ and $B_{\mu}^{(i)}$ ($i = 1.. \mu$)

$$\begin{aligned}
B_1^{(1)} &= a(2q_{\rightarrow} - 0.5), \quad \gamma_1^{(1)} = 1 \\
B_2^{(1)} &= a^2(0.5 - (2q_{\rightarrow} - 0.5)^2), \quad \gamma_2^{(1)} = 1 \\
B_2^{(2)} &= a^2(2q_{\rightarrow} - 0.5)^2, \quad \gamma_2^{(2)} = 2.
\end{aligned} \tag{27}$$

The only missing component for computation of the moments for QTM is Q_0 that determines Λ in Eq. (23) using Eq. (14). Q_0 depends on F_0 in a non-trivial fashion. Below we develop this dependence that is summarized in Eq. (38).

The return probability Q_0 is found by the means of generating functions [31]. We use the probability of first return to the starting point ($\mathbf{r} = 0$) after N steps, i.e., $f_N(0)$, and represent Q_0 as $Q_0 = \lim_{z \rightarrow 1} (\sum_{N=0}^{\infty} f_N(0)z^N)$. $p_N(0)$ is the probability to find the RW at position $\mathbf{r} = 0$ after N steps. The quantities $f_N(0)$ and $p_N(0)$ are related by [31]

$$\sum_{N=0}^{\infty} f_N(0)z^N = 1 - \frac{1}{\sum_{N=0}^{\infty} p_N(0)z^N} \quad (28)$$

which means that

$$Q_0 = 1 - \lim_{z \rightarrow 1} \frac{1}{(\sum_{N=0}^{\infty} p_N(0)z^N)}. \quad (29)$$

The term in the denominator in Eq. (29) is evaluated by calculating the Fourier transform of the jump probability of the RW, i.e., $\lambda(\mathbf{k}) = \langle \exp(i\mathbf{k} \cdot \mathbf{r}) \rangle_{RW}$, and taking the inverse Fourier transform of the sum of geometrical series, i.e.

$$I_z = \sum_{N=0}^{\infty} p_N(0)z^N = \frac{ab}{(2\pi)^2} \int_{-\pi/b}^{\pi/b} \int_{-\pi/a}^{\pi/a} \frac{d^2\mathbf{k}}{1 - z\lambda(\mathbf{k})}. \quad (30)$$

In the case of rectangular lattice, $\lambda(\mathbf{k})$ is a finite sum

$$\lambda(\mathbf{k}) = \langle e^{i\mathbf{k} \cdot \mathbf{r}} \rangle_{RW} = q_{\rightarrow} e^{i\tilde{k}_x} + (1/2 - q_{\rightarrow}) e^{-i\tilde{k}_x} + q_{\uparrow} e^{i\tilde{k}_y} + (1/2 - q_{\uparrow}) e^{-i\tilde{k}_y} \quad (31)$$

where we set for convenience the change of variables $\tilde{k}_x = ak_x$ and $\tilde{k}_y = bk_y$. We substitute $q_{\rightarrow} = \frac{1}{4}(1 + \tilde{F}_x)$ and $q_{\uparrow} = \frac{1}{4}(1 + \tilde{F}_y)$, that yields for Eq. (30)

$$I_z = \frac{1}{(2\pi)^2} \int_{-\pi}^{\pi} \int_{-\pi}^{\pi} \frac{d\tilde{k}_x d\tilde{k}_y}{1 - z \left[\frac{1}{2} \cos(\tilde{k}_x) + \frac{1}{2} \cos(\tilde{k}_y) + \frac{i}{2} (\tilde{F}_x \sin(\tilde{k}_x) + \tilde{F}_y \sin(\tilde{k}_y)) \right]}. \quad (32)$$

Note that when the external force $F_0 > 0$, this integral attains a final value in contrast to the unbiased case. That is why we can substitute $z = 1$ straight away before

explicitly evaluating the integral. Additionally, multiplying both the nominator and denominator by the conjugate of the denominator yields

$$I_1 = \frac{1}{(2\pi)^2} \int_{-\pi}^{\pi} \int_{-\pi}^{\pi} \frac{[1 - \frac{1}{2} \cos(\tilde{k}_x) - \frac{1}{2} \cos(\tilde{k}_y)] + \frac{i}{2} [\tilde{F}_x \sin(\tilde{k}_x) + \tilde{F}_y \sin(\tilde{k}_y)]}{[1 - \frac{1}{2} \cos(\tilde{k}_x) - \frac{1}{2} \cos(\tilde{k}_y)]^2 + \frac{1}{4} [\tilde{F}_x \sin(\tilde{k}_x) + \tilde{F}_y \sin(\tilde{k}_y)]^2} d\tilde{k}_x d\tilde{k}_y \quad (33)$$

Since we are looking for a strictly real solution, we can take only the real part of the integral, i.e.,

$$I_1 = \frac{1}{(2\pi)^2} \int_{-\pi}^{\pi} \int_{-\pi}^{\pi} \frac{\sin^2(\tilde{k}_x/2) + \sin^2(\tilde{k}_y/2)}{[\sin^2(\tilde{k}_x/2) + \sin^2(\tilde{k}_y/2)]^2 + \frac{1}{4} [\tilde{F}_x \sin(\tilde{k}_x) + \tilde{F}_y \sin(\tilde{k}_y)]^2} d\tilde{k}_x d\tilde{k}_y \quad (34)$$

Both the nominator and denominator are strictly positive, and the main contribution to the integral is from the area when both $k_x, k_y \rightarrow 0$. We approximate the solution by taking only the first terms in the Taylor series expansion of the trigonometric functions

$$I_1 = \frac{1}{(2\pi)^2} \int_{-\pi}^{\pi} \int_{-\pi}^{\pi} \frac{4(\tilde{k}_x)^2 + 4(\tilde{k}_y)^2}{[(\tilde{k}_x)^2 + (\tilde{k}_y)^2]^2 + 4[\tilde{F}_x \tilde{k}_x + \tilde{F}_y \tilde{k}_y]^2} d\tilde{k}_x d\tilde{k}_y. \quad (35)$$

By switching to polar coordinates $\rho = \sqrt{(\tilde{k}_x)^2 + (\tilde{k}_y)^2}$ and $\phi = \arctan(\tilde{k}_y/\tilde{k}_x)$:

$$\begin{aligned} I_1 &= \frac{1}{(2\pi)^2} \int_0^{2\pi} \int_0^{\pi\sqrt{2}} \frac{4\rho}{\rho^2 + 4(\tilde{F}_x \cos \phi + \tilde{F}_y \sin \phi)^2} d\rho d\phi \\ &= \frac{2}{(2\pi)^2} \int_0^{2\pi} \left[\ln [2\rho^2 + 4(\tilde{F}_x \cos \phi + \tilde{F}_y \sin \phi)^2] - \ln [4(\tilde{F}_x \cos \phi + \tilde{F}_y \sin \phi)^2] \right] d\phi. \end{aligned} \quad (36)$$

and taking the limit $F_0 \rightarrow 0$ we obtain that

$$I_1 \sim \frac{1}{\pi} \ln \left(\frac{2\pi^2}{(\tilde{F}_x)^2 + (\tilde{F}_y)^2} \right). \quad (37)$$

Finally, plugging this form of I_1 into Eq. (29), we find the dependence of the return probability on the force,

$$Q_0 = 1 + \pi \left[\ln \left(\frac{(\tilde{F}_x)^2 + (\tilde{F}_y)^2}{2\pi^2} \right) \right]^{-1} \text{ when } F_0 \rightarrow 0. \quad (38)$$

This result indicates that the return probability has a logarithmic dependence on F_0 .

Now we can finalize the calculation of the first and second moments for the QTM process. By plugging in the constants, $\gamma_\mu^{(i)}$, $B_\mu^{(i)}$ ($i = 1.. \mu$) found from Eq. (27) into Eq. (23) we obtain that for $0 < \alpha < 1$

$$\langle x \rangle_{QTM} = \frac{a}{2A\Gamma[1 + \alpha]} \frac{\tilde{F}_x}{\Lambda} t^\alpha \quad (39)$$

and

$$\langle x^2 \rangle_{QTM} = \frac{a^2}{2A\Gamma[1 + \alpha]} \left(1 - \frac{1}{2} (\tilde{F}_x)^2 \right) \frac{1}{\Lambda} t^\alpha + \frac{a^2}{2A^2\Gamma[1 + 2\alpha]} \frac{(\tilde{F}_x)^2}{\Lambda^2} t^{2\alpha} \quad (40)$$

while Λ is provided by Eq. (14) and Q_0 is the return probability given in Eq. (38).

For the case of a square lattice, we set the step lengths in both the x and y direction equal, hence $a = b$. Therefore for a square lattice, the return probability is

$$Q_0 = 1 + \frac{\pi}{2 \ln \left(a\tilde{F}_0 / (\sqrt{2}\pi) \right)} \quad (41)$$

where $\tilde{F}_0 = \frac{F_0}{2k_B T}$. This implies that for a square lattice, the return probability has no dependence on the direction of the force.

Our results show that the moments (Eq. (39-40)) have non-linear response both in time ($\langle x \rangle \sim t^\alpha$) and in the applied force. In particular, besides anomalous diffusion, the coefficients in both moments depend logarithmically on the external force applied through Λ . This is in contrast to CTRW, where the first and second moment has a coefficient that depends linearly on F_0 (in Sec.,V we will see the exact connection between CTRW and the QTM). The moments of x, y also show dependence on the

direction through the force term (\tilde{F}_x or \tilde{F}_y) and Q_0 (which determines Λ). This directional dependence will also appear in \mathbf{r} . In the case of the square lattice, the return probability (Q_0) does not depend on the direction of the force due to spatial symmetry, hence the moments of the displacement (\mathbf{r}) also do not depend on the direction of the applied force.

Our results are consistent with the expectation of unbiased scenario when $F_0 = 0$. By using the asymptotic relation $\text{Li}_{-\alpha}(Q_0) \sim \Gamma[1+\alpha](1-Q_0)^{-\alpha-1}$ [43] in Eq. (39) the limit of the unbiased case, i.e., $\langle x \rangle_{QTM} = 0$, is obtained in a straightforward manner. Note that the presented theory can be used to calculate the QTM's moments of any parameter (x , y or \mathbf{r}) by switching only the relevant constants for $B_\mu^{(i)}$ and $\gamma_\mu^{(i)}$ in Eq. (23) as we will see in the appendix (Sec. VII) for the cases of the oblique and hexagonal lattice types.

IV. SIMULATIONS

This section compares our analytical results to numerical simulations and discusses the numerical convergence to the theory.

For the theory to correctly represent the simulations, we need to run the simulations for a sufficiently large measurement time t . This is because the theory was developed for the regime when $t \rightarrow \infty$ and $S_\alpha \rightarrow \infty$ such that a convergence of S_α to ΛN (Eq. (13)) occurs (as can be seen in Fig. 3). This linear connection between S_α and Λ is achieved in the biased case when a sufficient number of returns of the RW to each site was performed. The RW must perform these returns; otherwise, the sites are not revisited, and the process will behave as CTRW, in contradiction to the theory. In other words, the correlations between various dwell times are essential for two-dimensional QTM. Therefore it is crucial to properly sample such events, i.e., observe enough returns of the RW. Since there are more degrees of freedom in 2d

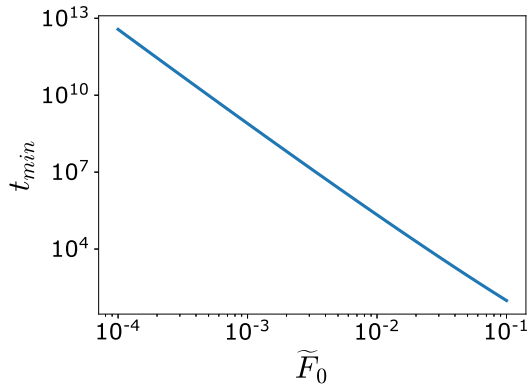


FIG. 2: The plot in the log-log scale of the minimal time (t_{min}) required for the theory to be a correct representation of the simulations as described by Eq. (44) vs. the force applied \tilde{F}_0 . The constants taken here are $\alpha = 0.5$, $A = 1$ and $\theta = \pi/4$.

The lattice type is a square with step size $a = 1$.

than in 1d, the time it takes to sample such events in 2d is significantly larger than in 1d (as was already mentioned in the introduction). Hence, for a given force F_0 , it takes much more steps of the RW in 2d (compared to 1d) to observe the convergence of S_α to the linear prediction. From these considerations, a logical approach is to define, at least qualitatively, minimum $t = t_{min}$, required for the theory (Eq. (39) and Eq. (40)) to be correct. Such a condition can be based on the physical intuition that the second moment $\langle x^2 \rangle_{QTM}$ should always be monotonically increasing with the external force F_0 . Hence, in the case of a rectangular lattice from the condition $\frac{\partial \langle x^2 \rangle}{\partial F_0} > 0$ we find that for small values of \tilde{F}_0

$$t^\alpha > \frac{A\Gamma[1 + 2\alpha]}{2a^2 \cos^2(\theta)\Gamma[1 + \alpha]} \frac{1}{\tilde{F}_0} \left(\frac{\partial \Lambda}{\partial \tilde{F}_0} \right) \quad (42)$$

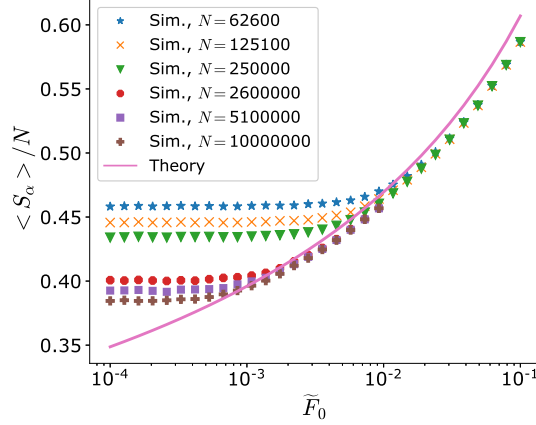


FIG. 3: Convergence of local time S_α to ΛN on a two-dimensional square lattice. Plot of simulation results of $\Lambda = \langle S_\alpha(N) \rangle / N$ for increasing values of N (number of steps) as a function of the force \tilde{F}_0 . The continuous line is the theoretical value of Λ in Eq. (14). The constants taken here are $\alpha = 0.5$, $A = 1$, $\theta = \pi/4$, $a = b = 1$ and the ensemble average is done on 10^3 independent RW's. Note that the difference between the theory and simulations in the range $\tilde{F}_0 > 10^{-2}$ stems from the fact that we evaluated analytically Λ (and its dependence on the return probability Q_0) in the limit $\tilde{F}_0 \rightarrow 0$. Also note that as N (number of steps) is increased we get a better agreement between theory and simulations for smaller values of \tilde{F}_0 . Taking larger values of N corresponds to larger values of measurement time t . The range of the plot corresponds to $Q_0 \sim 0.853$ ($\tilde{F}_0 = 10^{-4}$) and ~ 0.586 ($\tilde{F}_0 = 10^{-1}$).

where

$$\frac{\partial \Lambda}{\partial \tilde{F}_0} = \frac{2\pi(1-Q_0)}{\tilde{F}_0 \left(Q_0 \ln \left(\frac{a^2 \cos^2(\theta) + b^2 \sin^2(\theta)}{2\pi^2} (\tilde{F}_0)^2 \right) \right)^2} [Li_{-\alpha}(Q_0) - (1-Q_0)Li_{-\alpha-1}(Q_0)]. \quad (43)$$

Hence the measurement time t has to be larger then

$$t_{min}(\tilde{F}_0) = \left(\frac{A\Gamma[1+2\alpha]}{2a^2 \cos^2(\theta)\Gamma[1+\alpha]} \frac{1}{\tilde{F}_0} \left(\frac{\partial \Lambda}{\partial \tilde{F}_0} \right) \right)^{\frac{1}{\alpha}} \quad (44)$$

for the theory to be correct for values of the external force as small as \tilde{F}_0 . We can notice that this value diverges when $\theta = \pi/2$. This is the case when the external force is applied in the y direction, so the projection on the x axis is zero. In this case, the moments of x do not depend on the force, and we need to apply the same logic to obtain the moments of y instead. To see how t_{min} behaves, we plot its dependence on the force In Fig. 2. The asymptotic behavior of t_{min} when $F_0 \rightarrow 0$ is

$$t_{min} \sim \left(\tilde{F}_0 \left| \ln(\tilde{F}_0) \right| \right)^{-2/\alpha}, \quad \left(\tilde{F}_0 \rightarrow 0 \right) \quad (45)$$

as can also be verified in Fig. 2. It is also apparent from Eq. (44) that t_{min} decreases as α is closer to 1. This occurs since as $\alpha \rightarrow 1$ the system approaches the conditions when mean dwell times are finite. The time it takes S_α to converge to ΛN is displayed in Fig. 3. We can see that as the force (\tilde{F}_0) gets smaller, we need a larger amount of steps (N) for the convergence to take place. Taking a larger amount of steps corresponds to larger values of the measurement time (t). This can be seen from the PDF of t given in Eq. (8). Note that the difference in Fig. (3) between the theory and simulations in the range $\tilde{F}_0 > 10^{-2}$ stems from the fact that we evaluated Λ (and its dependence on the return probability Q_0) in the limit $\tilde{F}_0 \rightarrow 0$.

In Fig. 4 we compare theory and simulation results of the first and second moments of the QTM. For the value of measurement time t chosen in Fig. 4 ($t = 10^9$) the theory and simulations agree for values of \tilde{F}_0 as small as $\sim 3 \cdot 10^{-3}$. These forces and the measurement time (in Fig. 4) are consistent with Eq. (45).

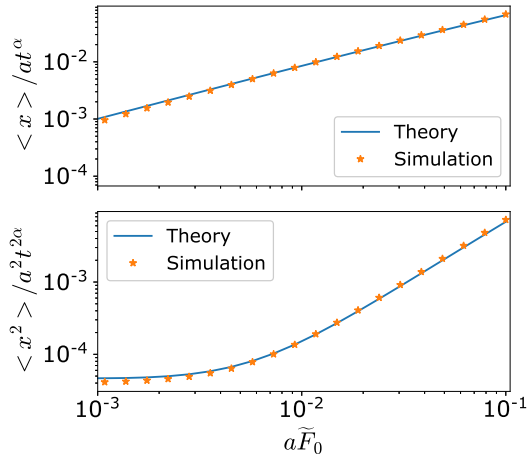


FIG. 4: A comparison between our theory and simulation results for the 2d QTM. In the top panel, we have a plot of the first moment and in the bottom the second moment. The lattice type taken here is a square with unit spacing ($a = 1$). The constants are $\alpha = 0.5$, $A = 1$, $t = 10^9$ and $\theta = \pi/4$. For each plot, the ensemble average is taken over 10^6 samples. For the chosen value of t ($t = 10^9$) we have an agreement with theory for values of \tilde{F}_0 as small as $\sim 10^{-3}$ (as explained in Sec. (IV) (Simulations)).

V. EQUIVALENCY BETWEEN THE QTM AND CTRW

In CTRW we have only one level of subordination since the local time is simply the step number N as compared to S_α in QTM. Then since the PDF of CTRW (Eq. (4)) is $\langle P(\mathbf{r}, t) \rangle_{CTRW} = \sum_N W_N(\mathbf{r}) \mathcal{P}_t(N)$ and $\mathcal{P}_t(N)$, the probability to observe N steps during time t is given in Eq. (3) we have

$$\langle P(\mathbf{r}, t) \rangle_{CTRW} \sim \int_0^\infty W_N(\mathbf{r}) \frac{t}{\alpha} N^{-1/\alpha-1} l_{\alpha, A, 1} \left(\frac{t}{N^{1/\alpha}} \right) dN \quad t \rightarrow \infty. \quad (46)$$

Comparing this equation of CTRW to that of QTM (Eq. (17)) yields the result

$$\langle P(\mathbf{r}, t) \rangle_{QTM} \sim \langle P(\mathbf{r}, t/\Lambda^{1/\alpha}) \rangle_{CTRW}, \quad t \rightarrow \infty \quad (47)$$

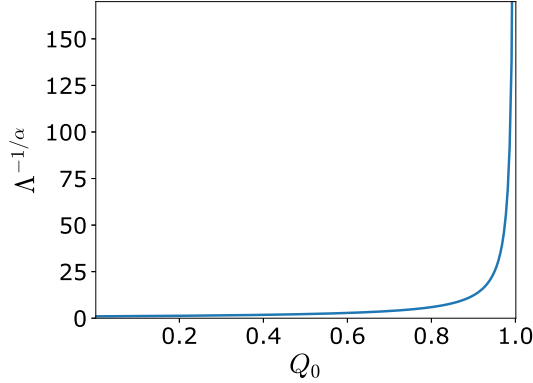


FIG. 5: A plot of the temporal transformation constant $1/\Lambda^{1/\alpha}$ that takes us from CTRW to the equivalent state in QTM for $\alpha = 0.5$ as a function of the return probability Q_0 . The divergence for $Q_0 \rightarrow 1$ signifies the limitation of this transformation strictly to the transient case. Note that $\Lambda = 1$ when $Q_0 \rightarrow 0$, i.e when the force F_0 is large enough.

meaning that the transformation

$$t \rightarrow t/\Lambda^{1/\alpha} \tag{48}$$

takes us from transient CTRW to the equivalent disorder averaged propagator in QTM. A plot of the constant ($1/\Lambda^{1/\alpha}$) is presented in Fig. 5. When $Q_0 = 0$ ($\Lambda = 1$), the QTM is exactly described by the CTRW since the walker never returns to a previously visited site. For any $0 < Q_0 < 1$ the constant ($\Lambda^{-1/\alpha}$) is greater than 1. This means that the limiting PDF attained in both models as $t \rightarrow \infty$ is achieved faster in the QTM than in the CTRW. The reason is that CTRW has a higher chance (compared to QTM) to roll a very large dwell time at each step (because we re-roll a new dwell time every step regardless of the position in space) and thus "waste" more time.

Furthermore, we compare this temporal mapping to the equivalent one in the

one-dimensional case. In the case of the biased 1d QTM, we know from [26] that the escape probability is

$$\tilde{Q}_0 = 2(1 - q) \quad (49)$$

where q is the bias in 1d to step right. From our definition of the force in 2d the applied force on the x axis is $\tilde{F}_x = a \cos(\theta) \tilde{F}_0$. By defining similarly the connection between the force and bias in 1d, we will obtain $q = \frac{1}{2}(1 + \tilde{F}_x)$, i.e., $\tilde{Q}_0 = 1 - \tilde{F}_x$. While in 2d, say for the square lattice, we obtained in Eq. (29) that the return probability is $Q_0 = 1 + 0.5\pi / \ln(a\tilde{F}_0/(\sqrt{2}\pi))$. The comparison of the transformation constant $1/\Lambda^{1/\alpha} = [Q_0/((1 - Q_0)^2 Li_{-\alpha}(Q_0))]^{1/\alpha}$ (from Eq. (14)) for the 1d case against the 2d square lattice case shows that for a given force \tilde{F}_0 , $1/\Lambda^{1/\alpha}$ is larger for the 1d case. Meaning that the attained limiting PDF, when $t \rightarrow \infty$, is reached faster for the QTM in 1d than in 2d when the same force \tilde{F}_0 is applied. This can be explained by the fact that in 2d, we have more degrees of freedom and thus, on average, during time t , the RW visits a larger amount of different sites and, in turn, have more chances to roll larger dwell times and "waste" more time. The re-visitation rate for 1d is higher than in 2d. It also answers why the 2d QTM is closer to its CTRW counterpart than to the 1d version.

VI. CONCLUSIONS

By using the method of double subordination and utilizing the local time S_α , we obtain the positional PDF for the two-dimensional biased QTM with external force F_0 . This PDF and the obtained return probability Q_0 allows us to write an explicit formula for the moments of the system on various lattice types in 2d. The moments show non-linear response both in time ($\langle x \rangle \sim t^\alpha$) and in the applied force. Our results are consistent with Ref., [44] which predicts non-self-averaging, characteristics of aging, and anomalous behavior when $\alpha < 1$, i.e., diverging mean dwell times. In

particular, besides anomalous behavior in time, our results show that the first and second moments depend logarithmically on the external force applied via the Λ term. This result is in contrast to the CTRW model, where the first moment has a coefficient that depends linearly on F_0 . The moments are also affected in a non-linear fashion by the direction of the applied force in each lattice type that was presented (rectangular, oblique, and hexagonal) except for the square lattice type, where the dependence is canceled out due to spatial symmetry. This again is in contrast to what is expected for the mean-field representation of CTRW [42]. These differences between QTM and CTRW appear despite the equivalence between the two models (when external bias is present) that is achieved via the temporal transformation $t \rightarrow t/\Lambda^{1/\alpha}$. The constant Λ depends on the direction and the size of the force \tilde{F}_0 in a non-linear fashion.

Quenched disorder and anomalous behavior of the dwell times induce the observed non-linear response, i.e., non-linear dependence of the average position on the size of the external field. The non-linear response and associated breaking of the Einstein relation were predicted for the 1d QTM using scaling arguments [2], and explicitly calculated in the limit of $T \rightarrow 0$ [20]. This non-linear response appears in 1d only for measurement times $t > (\tilde{F}_0)^{-1-1/\alpha}$ when $\tilde{F}_0 \rightarrow 0$ [2]. Our results (Eq. (45)) show that for the two-dimensional case the measurement time t for which the non-linear response reveals itself scales as $\left(\tilde{F}_0 \left|\ln(\tilde{F}_0)\right|\right)^{-2/\alpha}$. For any $0 < \alpha < 1$ the time-scales where non-linearity of response takes place is therefore significantly larger for the two-dimensional case. Since the QTM was developed as a toy model for glassy systems, this prediction of non-linear response to external force in 2d might be explored in situations where aging, quenched disorder, and anomalous behavior have been reported. Systems like Physical glasses [45, 46] and bio-materials [47, 48]. It is important to remember that our work suggests that this non-linearity will reveal itself only for a very long measurement time. The last thing to mention is that our

theory can be extended to other lattices in higher dimensions as long as the return probability Q_0 is known and smaller than one.

ACKNOWLEDGEMENTS

This work was supported by the Israel Science Foundation Grant No. 2796/20.

VII. APPENDIX

A. Appendix A - Oblique lattice

For the oblique lattice, we have a walker that can jump a distance of a in either direction on the x axis and a distance of b in either direction on the axis rotated by an angle of ϕ (relative to the x axis). An example of a general oblique lattice can be seen in Fig. 6 panel (1). Following the same logic as in the rectangular lattice type, the jumping probabilities for a single step on an oblique lattice are

$$\begin{aligned} q_a &= \frac{1}{4}(1 + \tilde{F}_a) \\ q_b &= \frac{1}{4}(1 + \tilde{F}_b) \\ q_{-a} &= \frac{1}{4}(1 - \tilde{F}_a) \\ q_{-b} &= \frac{1}{4}(1 - \tilde{F}_b) \end{aligned} \tag{50}$$

where from geometrical considerations, we have the bias in each direction

$$\begin{aligned} \tilde{F}_a &= \frac{aF_0}{2k_B T} \frac{\sin(\phi - \theta)}{\sin(\phi)} \\ \tilde{F}_b &= \frac{bF_0}{2k_B T} \frac{\sin(\theta)}{\sin(\phi)}. \end{aligned} \tag{51}$$

\tilde{F}_a is the bias in the direction of x and \tilde{F}_b is the bias in the direction of the step size b , i.e., in the direction of ϕ relative to the positive direction of x (see Fig. 6).

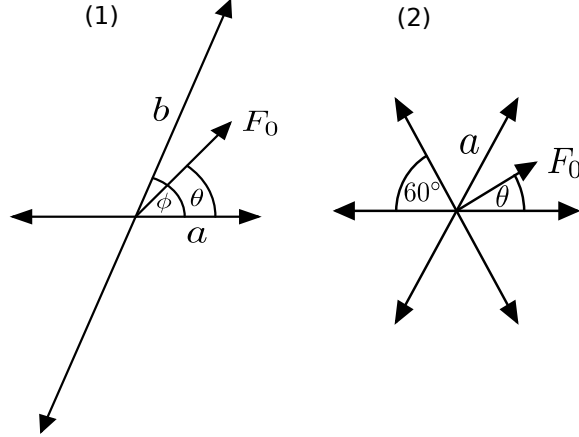


FIG. 6: A sketch of the two lattice types examples is discussed in this section. In panel (1), we have a general oblique lattice skewed by an angle of ϕ relative to the x axis. In panel (2), a hexagonal lattice type is sketched, the walker has at each new random step six evenly spaced out directions to choose from.

We repeat the same steps as in the rectangular lattice to calculate the return probability Q_0 of the oblique lattice. The characteristic function $\lambda(\mathbf{k}) = \langle \exp(i\mathbf{k} \cdot \mathbf{r}) \rangle$ in the case of the oblique lattice becomes

$$\begin{aligned} \lambda(\mathbf{k}) = & \frac{1}{4}(1 + F_a) \exp(iak_x) + \frac{1}{4}(1 - F_a) \exp(-iak_x) \\ & + \frac{1}{4}(1 + F_b) \exp(ib \cos(\phi)k_x + ib \sin(\phi)k_y) \\ & + \frac{1}{4}(1 - F_b) \exp(-ik_x b \cos(\phi) - ik_y b \sin(\phi)). \end{aligned} \quad (52)$$

Now transforming $\lambda(\mathbf{k})$ to trigonometric functions we receive

$$\begin{aligned} \lambda(\mathbf{k}) = & \frac{1}{2} \cos(ak_x) + \frac{1}{4}iF_a \sin(ak_x) \\ & + \frac{1}{2} \cos(ib \cos(\phi)k_x + ib \sin(\phi)k_y) + \frac{1}{2} \cos(ib \cos(\phi)k_x + ib \sin(\phi)k_y). \end{aligned} \quad (53)$$

Our boundaries in this case are $|x| < \max\{a, b \cos(\phi)\}$ since the projection of b onto the x axis can be larger than the step size a on the x axis and $|y| < b \sin(\phi)$. The

integral we need to evaluate in Eq. (30) is now

$$I_z = \frac{cb \sin(\phi)}{4\pi^2} \int_{-\frac{\pi}{b \sin(\phi)}}^{\frac{\pi}{b \sin(\phi)}} \int_{-\pi/c}^{\pi/c} \frac{dk_x dk_y}{1 - z\lambda(k_x, k_y)} \quad (54)$$

where we set $c = \max\{a, b \cos(\phi)\}$. By using Taylor expansion in the $k_x, k_y \rightarrow 0$ limit and substituting $z = 1$, Eq. (54) becomes

$$I_1 = \frac{cb \sin(\phi)}{4\pi^2} \int_{-\frac{\pi}{b \sin(\phi)}}^{\frac{\pi}{b \sin(\phi)}} \int_{-\pi/c}^{\pi/c} \frac{dk_x dk_y \left[(ak_x/2)^2 + (\vec{k} \cdot \vec{b}/2)^2 \right]}{\left[(ak_x/2)^2 + (\vec{k} \cdot \vec{b}/2)^2 \right]^2 + \left(a\tilde{F}_a k_x/2 + \tilde{F}_b \vec{k} \cdot \vec{b}/2 \right)^2}. \quad (55)$$

Changing variables $\tilde{k}_x = ak_x$ and $\tilde{k}_y = k_x b \cos(\phi) + k_y b \sin(\phi)$ the Jacobian becomes $J = 1/(ab \sin(\phi))$ and I_1 is transformed to

$$I_1 = \frac{c}{4\pi^2 a} \int_{-\pi - \pi b \cos(\phi)/c}^{\pi + \pi b \cos(\phi)/c} \int_{-a\pi/c}^{a\pi/c} \frac{4(\tilde{k}_x)^2 + 4(\tilde{k}_y)^2}{\left[(\tilde{k}_x)^2 + (\tilde{k}_y)^2 \right]^2 + 4[\tilde{F}_x \tilde{k}_x + \tilde{F}_y \tilde{k}_y]^2} d\tilde{k}_x d\tilde{k}_y. \quad (56)$$

By switching to polar coordinates and taking the limit $F_0 \rightarrow 0$, we obtain

$$I_1 = \frac{c}{a\pi} \ln \left(\frac{\left(\frac{a\pi}{c} \right)^2 + \pi^2 \left(1 + \frac{b \cos(\phi)}{c} \right)^2}{(\tilde{F}_a)^2 + (\tilde{F}_b)^2} \right) \quad (57)$$

and since $Q_0 = 1 - 1/I_1$ the final form for the return probability in the $F_0 \rightarrow 0$ limit is

$$Q_0 = 1 + \frac{a\pi}{c} \left[\ln \left(\frac{(\tilde{F}_a)^2 + (\tilde{F}_b)^2}{\left(\frac{a\pi}{c} \right)^2 + \pi^2 \left(1 + \frac{b \cos(\phi)}{c} \right)^2} \right) \right]^{-1} \quad (F_0 \rightarrow 0). \quad (58)$$

Now that we know the return probability Q_0 , we have the value of Λ from Eq. (14). All we require now to have the value of the moments are the constants of the spatial processes $\gamma_\mu^{(i)}$, $B_\mu^{(i)}$ ($i = 1.. \mu$) for the case of the oblique lattice. After we find these constants, we plug them into Eq. (23) and acquire the moments.

We now continue to find the constants of the spatial processes. The average displacement after N steps is related to a single step displacement l_x by $\langle x \rangle = N \langle l_x \rangle$,

from here we find

$$\langle x \rangle_{RW} = (2a\tilde{F}_a + 2\cos(\phi)b\tilde{F}_b)N. \quad (59)$$

And since the steps are independent of each other (Markovian process) the variance of the position x after N steps is related to the variance of a single step displacement l_x by $\text{Var}(x) = N\text{Var}(l_x)$. The second moment of the spatial process now becomes

$$\begin{aligned} \langle x^2 \rangle_{RW} = & \left[\left(\frac{1}{2}a^2 + \frac{1}{2}b^2 \cos^2(\phi) \right) - \left(2a\tilde{F}_a + 2\cos(\phi)b\tilde{F}_b \right)^2 \right] N \\ & + \left[2a\tilde{F}_a + 2\cos(\phi)b\tilde{F}_b \right]^2 N^2 \end{aligned} \quad (60)$$

Comparison of Eq. (19) to Eqs. (59,60) yields for $\gamma_\mu^{(i)}$ and $B_\mu^{(i)}$ ($i = 1.. \mu$)

$$\begin{aligned} B_1^{(1)} &= 2a\tilde{F}_a + 2\cos(\phi)b\tilde{F}_b, \quad \gamma_1^{(1)} = 1 \\ B_2^{(1)} &= \left(\frac{1}{2}a^2 + \frac{1}{2}b^2 \cos^2(\phi) \right) - \left(2a\tilde{F}_a + 2\cos(\phi)b\tilde{F}_b \right)^2, \quad \gamma_2^{(1)} = 1 \\ B_2^{(2)} &= (2a\tilde{F}_a + 2\cos(\phi)b\tilde{F}_b)^2, \quad \gamma_2^{(2)} = 2. \end{aligned} \quad (61)$$

This concludes the case of the oblique lattice.

B. Appendix B - Hexagonal lattice

We perform the same steps as in the rectangular lattice to explicitly calculate the return probability for the hexagonal lattice. The hexagonal lattice has six symmetrical jump directions of size a in each step (as sketched in Fig. 6 panel (2)), the characteristic function $\lambda(\mathbf{k}) = \langle \exp(i\mathbf{k} \cdot \mathbf{r}) \rangle$ becomes

$$\begin{aligned} \lambda(\mathbf{k}) = & \frac{1}{6}(1 + \tilde{F}_a) \exp(iak_x) + \frac{1}{6}(1 - \tilde{F}_a) \exp(-iak_x) + \frac{1}{6}(1 + \tilde{F}_b) \exp\left(i\frac{a}{2}k_x + i\frac{\sqrt{3}a}{2}k_y\right) \\ & + \frac{1}{6}(1 - \tilde{F}_b) \exp\left(-i\frac{a}{2}k_x - i\frac{\sqrt{3}a}{2}k_y\right) + \frac{1}{6} \exp\left(-i\frac{a}{2}k_x + i\frac{\sqrt{3}a}{2}k_y\right) \\ & + \frac{1}{6} \exp\left(i\frac{a}{2}k_x - i\frac{\sqrt{3}a}{2}k_y\right) \end{aligned} \quad (62)$$

where from geometrical considerations, we have

$$\begin{aligned}\tilde{F}_a &= \left(\cos(\theta) - \frac{1}{\sqrt{3}} \sin(\theta) \right) \frac{aF_0}{2k_B T} \\ \tilde{F}_b &= \frac{aF_0 \sin(\theta)}{\sqrt{3}k_B T}.\end{aligned}\tag{63}$$

\tilde{F}_a is the bias in the direction of x and \tilde{F}_b is in the direction of 60° relative to the positive direction of x (see Fig. 6). Now transforming $\lambda(\mathbf{k})$ to trigonometric functions we receive

$$\begin{aligned}\lambda(\mathbf{k}) &= \frac{1}{3} \cos(ak_x) + \frac{1}{3} i \tilde{F}_a \sin(ak_x) + \frac{1}{3} \cos\left(\frac{1}{2}ak_x + \frac{\sqrt{3}}{2}ak_y\right) \\ &+ \frac{1}{3} i \tilde{F}_b \sin\left(\frac{1}{2}ak_x + \frac{\sqrt{3}}{2}ak_y\right) + \frac{1}{3} \cos\left(\frac{1}{2}ak_x - \frac{\sqrt{3}}{2}ak_y\right).\end{aligned}\tag{64}$$

Since our boundaries are $-a < x < a$ and $-\frac{\sqrt{3}a}{2} < y < \frac{\sqrt{3}a}{2}$ the integral we need to evaluate is

$$I_z = \frac{\sqrt{3}a^2}{8\pi^2} \int_{-\frac{2\pi}{\sqrt{3}a}}^{\frac{2\pi}{\sqrt{3}a}} \int_{-\pi/a}^{\pi/a} \frac{dk_x dk_y}{1 - z\lambda(k_x, k_y)}.\tag{65}$$

By using Taylor expansion in the $k_x, k_y \rightarrow 0$ limit, substituting $z = 1$ and setting $\tilde{k}_x = ak_x$, $\tilde{k}_y = ak_y$, Eq. (65) is transformed into

$$I_1 = \frac{\sqrt{3}}{8\pi^2} \int_{-\frac{2\pi}{\sqrt{3}}}^{\frac{2\pi}{\sqrt{3}}} \int_{-\pi}^{\pi} \frac{4d\tilde{k}_x d\tilde{k}_y (\tilde{k}_x^2 + \tilde{k}_y^2)}{(\tilde{k}_x^2 + \tilde{k}_y^2)^2 + \frac{64}{36} \left((\tilde{F}_a + \frac{1}{2}\tilde{F}_b) \tilde{k}_x + \frac{\sqrt{3}}{2}\tilde{F}_b \tilde{k}_y \right)^2}.\tag{66}$$

By switching to polar coordinates and taking the limit $F_0 \rightarrow 0$ we obtain

$$I_1 = \frac{\sqrt{3}}{2\pi} \ln \left[\frac{21\pi^2/4}{(\tilde{F}_a)^2 + (\tilde{F}_b)^2 + \tilde{F}_a \tilde{F}_b} \right].\tag{67}$$

Since $Q_0 = 1 - 1/I_1$ the final form for the return probability in the $F_0 \rightarrow 0$ limit is:

$$Q_0 = 1 + \frac{2\pi}{\sqrt{3}} \left[\ln \left(\frac{(\tilde{F}_a)^2 + (\tilde{F}_b)^2 + \tilde{F}_a \tilde{F}_b}{21\pi^2/4} \right) \right]^{-1} \quad (F_0 \rightarrow 0).\tag{68}$$

To obtain the the moments of QTM on a hexagonal lattice, constants of the spatial processes $\gamma_\mu^{(i)}, B_\mu^{(i)}$ ($i = 1..\mu$) are needed. Following the same logic as before, we receive

$$\langle x \rangle_{RW} = (2a\tilde{F}_a + a\tilde{F}_b)N \quad (69)$$

and

$$\langle x^2 \rangle_{RW} = \left[\frac{1}{2}a^2 - (2a\tilde{F}_a + a\tilde{F}_b)^2 \right] N + (2a\tilde{F}_a + a\tilde{F}_b)^2 N^2. \quad (70)$$

Comparison of Eq. (19) to Eqs. (69,70) yields for $\gamma_\mu^{(i)}$ and $B_\mu^{(i)}$ ($i = 1..\mu$)

$$\begin{aligned} B_1^{(1)} &= 2a\tilde{F}_a + a\tilde{F}_b, \quad \gamma_1^{(1)} = 1 \\ B_2^{(1)} &= \frac{1}{2}a^2 - (2a\tilde{F}_a + a\tilde{F}_b)^2, \quad \gamma_2^{(1)} = 1 \\ B_2^{(2)} &= (2a\tilde{F}_a + a\tilde{F}_b)^2, \quad \gamma_2^{(2)} = 2. \end{aligned} \quad (71)$$

This concludes the case of the hexagonal lattice.

VIII. BIBLIOGRAPHY

- [1] S. Alexander, J. Bernasconi, W. R. Schneider, and R. Orbach *Excitation dynamics in random one-dimensional systems*, Rev. Mod. Phys. **53**, 175 (1981).
- [2] J. P. Bouchaud and A. Georges, *Anomalous diffusion in disordered media: Statistical mechanisms, models and physical applications*, Phys. Rep. **195**, 127 (1990).
- [3] R. Metzler and J. Klafter *The random walk's guide to anomalous diffusion: a fractional dynamics approach*, Phys. Rep. **339**, 1 (2000).
- [4] E. Barkai, Y. Garini, and R. Metzler, *Strange kinetics of single molecules in living cells*, Phys. Today **65**(8), 29 (2012).
- [5] S. M. A. Tabei, S. Burov, H. Y. Kim, A. Kuznetsov, T. Huynh, J. Jureller, L. H. Philipson, A. R. Dinner, and N. F. Scherer, *Intracellular transport of insulin granules is a subordinated random walk*, Proc. Natl. Acad. Sci. USA **110**, 4911 (2013).
- [6] F. D. Stefani, J. P. Hoogenboom, and E. Barkai, *Beyond quantum jumps: Blinking nanoscale light emitters*, Phys. Today **62**(2), 34 (2009).
- [7] M. Scholz, S. Burov, K. L. Weirich, B. J. Scholz, S. M. A. Tabei, M. L. Gardel, and A. R. Dinner, *Cycling State that Can Lead to Glassy Dynamics in Intracellular Transport*, Phys. Rev. X **6**, 011037 (2016).
- [8] H. Scher and E. W. Montroll, *Anomalous transit-time dispersion in amorphous solids*, Phys. Rev. B **12**, 2455 (1975).
- [9] J. P. Bouchaud, *Weak ergodicity breaking and aging in disordered systems*, J. Phys. I (France) **2**, 1705 (1992).
- [10] C. Monthus and J.-P. Bouchaud, *Models of traps and glass phenomenology*, J. Phys. A **29**, 3847 (1996).

- [11] B. Rinn, P. Maass, and J. P. Bouchaud, *Multiple Scaling Regimes in Simple Aging Models*, Phys. Rev. Lett. **84**, 5403 (2000).
- [12] B. Rinn, P. Maass, and J. P. Bouchaud, *Hopping in the glass configuration space: Subaging and generalized scaling laws*, Phys. Rev. B **64**, 104417 (2001).
- [13] L. Berthier and G. Biroli, *Theoretical perspective on the glass transition and amorphous materials*, Rev. Mod. Phys. **83**, 587 (2011).
- [14] M. F. Shlesinger, *Asymptotic solutions of continuous-time random walks*, J. Stat. Phys. **10**, 421 (1974).
- [15] J. Klafter and R. Silbey, *Derivation of the Continuous-Time Random-Walk Equation*, Phys. Rev. Lett. **44**, 55 (1980).
- [16] H. Scher, M. F. Shlesinger, and J. T. Bendler, *Time-Scale Invariance in Transport and Relaxation*, Phys. Today **44**(1), 26 (1991).
- [17] G. Bel and E. Barkai, *Weak Ergodicity Breaking in the Continuous-Time Random Walk*, Phys. Rev. Lett. **94**, 240602 (2005).
- [18] Y. He, S. Burov, R. Metzler, and E. Barkai, *Random Time-Scale Invariant Diffusion and Transport Coefficients*, Phys. Rev. Lett. **101**, 058101 (2008).
- [19] J Machta, *Random walks on site disordered lattices*, J. Phys. A **18**, L531 (1985).
- [20] C. Monthus, *Anomalous diffusion, localization, aging, and subaging effects in trap models at very low temperature*, Phys. Rev. E **68**, 036114 (2003).
- [21] Ben Arous, G., Černý, J. and Mountford, T. *Aging in two-dimensional Bouchaud's model.*, Probab. Theory Relat. Fields **134**, 1–43 (2006).
- [22] Gérard Ben Arous. Jiří Černý. *Scaling limit for trap models on \mathbb{Z}^d* . Ann. Probab. **35** (6) 2356 - 2384, November 2007.
- [23] Gérard Ben Arous. Manuel Cabezas. Jiří Černý. Roman Royfman. *Randomly trapped random walks*. Ann. Probab. **43** (5) 2405 - 2457, September 2015.
- [24] J. Černý and T. Wassmer, *Randomly trapped random walks on \mathbb{Z}^d* . Stoch. Proc. Their

- Appl. **125**, 1032 (2015).
- [25] S. Burov, *From quenched disorder to continuous time random walk*. Phys. Rev. E **96**, 050103(R) (2017).
- [26] S. Burov, *The transient case of the quenched trap model*. J. Stat. Mech. (2020) 073207.
- [27] Carsten F. E. Schroer and Andreas Heuer, *Anomalous Diffusion of Driven Particles in Supercooled Liquids*. Phys. Rev. Lett. **110**, 067801 (2013).
- [28] M. Khoury, A. M. Lacasta, J. M. Sancho, and Katja Lindenberg, *Weak Disorder: Anomalous Transport and Diffusion Are Normal Yet Again*. Phys. Rev. Lett. **106**, 090602 (2011).
- [29] O. Bénichou, A. Bodrova, D. Chakraborty, P. Illien, A. Law, C. Mejía-Monasterio, G. Oshanin, and R. Voituriez, *Geometry-Induced Superdiffusion in Driven Crowded Systems*. Phys. Rev. Lett. **111**, 260601 (2013).
- [30] J. R. Gomez-Solano, A. Blokhuis, and C. Bechinger, *Dynamics of Self-Propelled Janus Particles in Viscoelastic Fluids*. Phys. Rev. Lett. **116**, 138301 (2016).
- [31] Weiss, G.H., *Aspects and Applications of the Random Walk*. North Holland, Amsterdam (1994).
- [32] A. I. Saichev and G. M. Zaslavsky, *Fractional kinetic equations: solutions and applications*. Chaos **7**, 753 (1997).
- [33] E. Barkai, *Fractional Fokker-Planck equation, solution, and application*. Phys. Rev. E **63**, 046118 (2001).
- [34] M. M. Meerschaert and H.-P. Scheffler, *Limit theorems for continuous-time random walks with infinite mean waiting times*. J. Appl. Probab. **41**, 623 (2004).
- [35] I. M. Sokolov and J. Klafter, *From diffusion to anomalous diffusion: A century after Einstein's Brownian motion*. Chaos **15**, 026103 (2005).
- [36] S. B. Yuste and K. Lindenberg, *Trapping reactions with subdiffusive traps and particles characterized by different anomalous diffusion exponents*. Phys. Rev. E **72**, 061103

(2005).

- [37] S. Burov and E. Barkai, *Weak subordination breaking for the quenched trap model*. Phys. Rev. E **86**, 041137 (2012).
- [38] S. Burov and E. Barkai, *Time Transformation for Random Walks in the Quenched Trap Model*. Phys. Rev. Lett. **106**, 140602 (2011).
- [39] E. M. Bertin and J.-P. Bouchaud, *Subdiffusion and localization in the one-dimensional trap model*. Phys. Rev. E **67**, 026128 (2003).
- [40] C. Monthus, *Non-linear response of the trap model in the aging regime: Exact results in the strong-disorder limit*. Phys. Rev. E **69**, 026103 (2004).
- [41] D. Schwarcz and S. Burov, *The effect of disordered substrate on crystallization in 2D*. J. Phys.: Condens. Matter **31** 445401 (2019).
- [42] J. Klafter and I. M. Sokolov, *First Steps in Random Walks: From Tools to Applications*, Oxford University Press (2011).
- [43] M. Abramowitz and I. A. Stegun, *Handbook of Mathematical Functions* (Dover Publications, New York, 1972).
- [44] T. Akimoto and K. Saito, *Trace of anomalous diffusion in a biased quenched trap model*. Phys. Rev. E **101**, 042133 (2020).
- [45] A. Amir, Y. Oreg and Y. Imry, *On relaxations and aging of various glasses*. Proc. Natl. Acad. Sci. **109**. 1850 (2012).
- [46] F. Arceri, F. Landes, L. Berthier, and G. Biroli, *Glasses and aging: A Statistical Mechanics Perspective*. hal-02942375f (2020).
- [47] S. Sadegh, J. L. Higgins, P. C. Mannion, M. M. Tamkun, and D. Krapf, *Plasma membrane is compartmentalized by a self-similar cortical actin meshwork*. Phys. Rev. X **7**, 011031 (2017).
- [48] J. Ślęzak and S. Burov, *From diffusion in compartmentalized media to non-Gaussian random walks*. Sci Rep **11**, 5101 (2021).